Applied Physics Letters

Effect of electric-field on the perpendicular magnetic anisotropy and strain properties in CoFeB/MgO magnetic tunnel junctions

Cite as: Appl. Phys. Lett. **105**, 052403 (2014); https://doi.org/10.1063/1.4892410
Submitted: 16 April 2014 . Accepted: 17 July 2014 . Published Online: 05 August 2014

V. B. Naik, H. Meng, J. X. Xiao, R. S. Liu, A. Kumar, K. Y. Zeng, P. Luo, S. Yap, et al.

Effect of electric-field on the perpendicular magnetic anisotropy and strain properties in CoFeB/MgO magnetic tunnel junctions

V. B. Naik,[1,a),b)] H. Meng,[1,b)] J. X. Xiao,[2] R. S. Liu,[1,c)] A. Kumar,[2] K. Y. Zeng,[2] P. Luo,[1] and S. Yap[1]

[1]*Data Storage Institute, A*STAR (Agency for Science Technology and Research), 5 Engineering Drive 1, DSI Building, Singapore 117608, Singapore*

[2]*Department of Mechanical Engineering, National University of Singapore, 9 Engineering Drive 1, Singapore 117576, Singapore*

(Received 16 April 2014; accepted 17 July 2014; published online 5 August 2014)

In this article, we investigate the effect of electric-field on the perpendicular magnetic anisotropy (PMA) and strain properties in nanoscaled CoFeB/MgO magnetic tunnel junction using tunnel magnetoresistance and piezoresponse force microscopy (PFM) measurements, respectively. We show that while the PMA change under electric-field is consistent with the previous reports, the PFM data show that the applied electric-field induces strain in a nanoscaled MgO. We demonstrate that the development of compressive and tensile strains corresponding to different polarities of applied electric-field. We discuss the interplay between the electric-field controlled PMA and strain properties. Our results may accelerate the development of magnetoelectrically controlled spintronic devices for low-power and high-density magnetic data storage applications. © *2014 AIP Publishing LLC*. [http://dx.doi.org/10.1063/1.4892410]

The magnetic tunnel junctions (MTJs) with MgO barriers have piqued the interest of researchers worldwide because it can have extremely large tunnel magnetoresistance (TMR).[1–6] Currently, the spin-transfer-torque (STT) switched MTJ based on CoFeB/MgO with perpendicular magnetic anisotropy (PMA) is regarded as a promising building block for the future high density magnetic random access memories (MRAM) due to its extremely large TMR ratio and a low threshold current density (J_C) for STT switching.[5–9] However, the writing power consumption of these MTJs is still a few orders larger than that of volatile semiconductor memories used in current integrated circuits.[10,11] Recently, it has been shown that an applied electric-field (*E*-field) can control the magnetic properties of 3*d* ferromagnets, and it is a promising alternative energy-efficient route to manipulate the magnetization of nanosized magnetic cells in MTJs compared to STT switching. These include studies on the *E*-field controlled interfacial magnetic anisotropy in thin film metallic ferromagnets,[12–15] magnetization control in ferromagnetic semiconductors[16] and the gate voltage controlled magnetic states in ferromagnetic field-effect devices.[17]

A most remarkable result is the recent demonstration of *E*-field-assisted reversible switching of magnetization in CoFeB/MgO MTJs with interfacial PMA at much lower current densities ($J_c \sim 10^4$ A/cm^2) as compared to STT switching.[18–21] The dramatic variation of PMA under the influence of *E*-field is attributed to the accumulation of charges at the ferromagnet/dielectric interface.[13] However, there is no consensus whether the charge accumulation or other undiscovered mechanisms exist. Generally, the *E*-field control of magnetic anisotropy is observed in single-phase multiferroics, which can exhibit simultaneously electric and magnetic orders[22–24] or in magnetoelectric (ME) composite nanostructures via strain-mediated cross interaction between the magnetostrictive effect in the ferromagnetic phase and piezoelectric effect in the ferroelectric/piezoelectric phase.[25–27] In ultrathin films of (Fe, Co, CoFeB)/MgO, the ferromagnet/dielectric interface plays a major role as compare to the bulk effect. At the interface, the atomic orbits of metal and O atoms hybridize and form metal-O bonds resulting in elastic distortion of the crystal lattice of the ferromagnet and MgO, which can induce a tensile strain.[28–30] It has been proposed that the applied *E*-field can displace O atom at the metal–O interface in high ionic mobility oxides.[31] Recently, using molecular dynamics simulation, Enyashin and Ivanovskii,[32] showed that the structure of nano-scaled MgO can be changed from cubic phase to non-cubic phase by applying a mechanical strain. Gopal and Spaldin theoretically predicted[33] that the structurally relaxed MgO can show piezoelectricity with piezoelectric constant as high as $e_{33} = 2.26$ C/m^2, yet there has been no experimental evidence of piezoelectric effect in nanoscaled MgO so far.

To gain more insight into the effect of strain on PMA properties of CoFeB/MgO MTJ under the influence of applied *E*-field, we have investigated the *E*-field effect in MTJ devices and *E*-field-induced strain effect in MgO nanostructures by performing TMR and piezoresponse force microscopy (PFM) measurements, respectively. The change in coercive field (H_C) under the *E*-field is consistent with other reports; however, our PFM results show that the applied *E*-field induces strain in a nanoscaled MgO. A detailed PFM measurements of the influence of polarity of *E*-field in nanoscaled MgO demonstrate that the development of compressive and tensile strains indicating that MgO exhibits a piezoelectric property at nanoscale. Our results will shed light on understanding the recently observed *E*-field-controlled PMA properties in CoFeB/MgO

[a)]Email: vinuprl@yahoo.com

[b)]Present address: GLOBALFOUNDRIES, 60 Woodlands Industrial Park D Street 2, Singapore, 738406.

[c)]Present address: Western Digital Corp., 44100 Osgood Road, Fremont, California 94539, USA.

MTJs,[18–20,34] and it may accelerate the development of energy efficient and high density magnetic data storage.

We have designed and fabricated two different stack structures: (1) To achieve *E*-field controlled PMA in MgO-CoFeB MTJs and (2) to investigate the *E*-field-induced strain effects in nanoscaled MgO so as to demonstrate its implication to the *E*-field controlled PMA. To investigate the effect of *E*-field on the PMA properties of CoFeB free layer (FL), the MTJ stacks were deposited on thermally oxidized Si substrate at room temperature with structure Si/SiO_2/bottom electrode/Ta2/CoFeB1/MgO2/CoFeB1.5/Ta5/Ru10 (numbers are nominal thicknesses in nanometres), where the composition of CoFeB is $Co_{40}Fe_{40}B_{20}$. The multilayer was processed into circular MTJ devices of 85 nm diameter (Fig. 1(a)) by electron beam lithography (EBL) and ion beam etching processes, and annealed in a vacuum oven at 300 °C for 1 h. The TMR loops were measured at room temperature with d.c. voltage (V_{DC}) under a perpendicular scanning magnetic field (H_{DC}). Here, the positive bias voltage is defined as inducing the tunnelling of electrons from the bottom CoFeB electrode to the top CoFeB electrode. Fig. 1(b) shows the minor TMR loops at selected V_{DC} values ($V_{DC} = -1$ V–1 V), which reveals a strong *E*-field-controlled PMA or H_C change, and the PMA becomes stronger under positive bias voltages ($V_{DC} > 0$), while it reduces under negative bias voltages ($V_{DC} < 0$ V). The increased H_C at positive V_{DC} and decreased H_C at negative V_{DC} (inset in Fig. 1(b)) are consistent with the previous reports.[18–20,34]

To study the *E*-field-induced strain effects in MgO nanostructures using PFM, a multilayer stack with bottom electrode/Ta5/CoFeB1/MgO5/Ta5/Ru5 (numbers are nominal thicknesses in nanometres) was deposited on oxidized Si substrate. A thicker MgO of 5 nm was used for PFM study to have larger signal than the sensitivity level of PFM. The thickness of top layer above the MgO layer was limited to 10 nm so that the induced strain can be measured using PFM along the direction perpendicular to the multilayers plane. The multilayer was patterned into circular nanopillars of diameter 800 nm by EBL and ion beam etching processes. The etched nanopillars were covered with SiO_2 and the top electrode was kept uncovered in order to apply the *E*-field in PFM measurement (Fig. 2(a)). Fig. 2(b) shows the AFM image of the patterned nanopillar devices. A bigger diameter of 800 nm was chosen to pattern the nanopillars such that PFM tip can safely placed on top surface of the nanopillar during scanning. Patterned nanopillar devices were annealed in a vacuum oven at 300 °C for 1 h. A commercial scanning probe microscopy (SPM) system (MFP-3D, Asylum Research, USA) was used with a commercial software platform (IGOR PRO 6.12A) and SPM control software (Asylum Research, version 090909–1214) to measure the *E*-field-induced strain in patterned MgO nanopillars. For quantitative characterization of the electromechanical properties, the dual AC resonance tracking (DART) PFM mode, which oscillates the conductive cantilever with two frequencies near the contact resonance frequency, was used. An a.c. voltage ranged from 1 to 2.5 V was applied between the tip and the nanopillar device to determine the strain coefficient (d_{zz}) versus V_{AC}. In order to study the effect of d.c. bias voltage (V_{DC}) on d_{zz}, a series of d.c. bias voltages ranged from $V_{DC} = -1.5$ V to 1.5 V, and an a.c. voltage of $V_{AC} = 0.3$ V were applied simultaneously to the tip by connecting the device bottom electrode to ground. The value of d_{zz} as a function of V_{DC} is determined by setting the d_{zz} of the unbiased ($V_{DC} = 0$) region to 0 pm. Here, the positive and negative d_{zz} values indicate the expansion (tensile strain) and contraction (compressive strain) of the material. In all PFM measurements, the Pt-coated Si tips (AC240TM, Olympus, Japan) with average tip radius of 15 nm, nominal stiffness of 2 N/m, and resonance frequency of 70 kHz were used. The line scan frequency used was 1 Hz.

Figs. 3(a) and 3(b) show the PFM images of the device under the applied a.c. voltage of amplitude 1 V and 2 V, respectively. Both the images show a clear color contrast between the circled and the rest areas with an enhancement for the higher applied voltage, indicating the development of strain under applied voltage in nanoscaled MgO and it becomes stronger as the voltage increases. In Fig. 3(c), we show the strain coefficient values (d_{zz}) at several voltage amplitudes and an approximately linear dependence of d_{zz} on voltage can be observed. The average value of d_{zz} determined from the slope of d_{zz} versus applied voltage is found to be $d_{zz} \approx 37$ pm/V. The increasing magnitude of d_{zz} with increasing *E*-field confirms that the applied *E*-field induces a

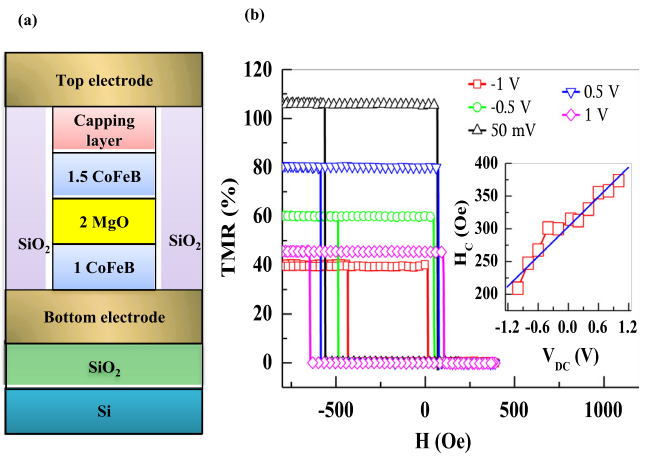

FIG. 1. Electric-field effect in CoFeB/MgO/CoFeB MTJ device with interfacial PMA. (a) Schematic drawing of a MTJ device. (b) Minor TMR loops of junction with 1.5 nm top CoFeB FL at different applied d.c. bias voltages ($V_{DC} = -1$ V–1 V). The inset shows the H_C as a function of applied d.c. bias voltage.

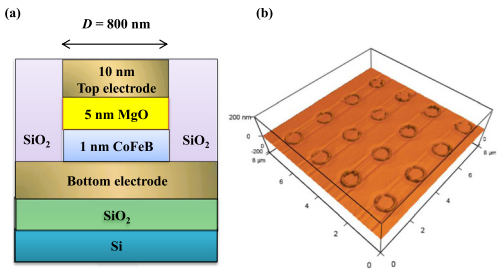

FIG. 2. Patterned nanopillar device with 5 nm MgO layer using electron beam lithography and etching processes for PFM study. (a) Schematic drawing of a patterned nanopillar device of diameter 800 nm with structure: bottom contact/1.2 nm CoFeB/5 nm MgO/10 nm top contact for PFM study. (b) Topography of nanopillar devices. Circles refers to the over filled SiO_2 around the edge of a patterned nanopillar device.

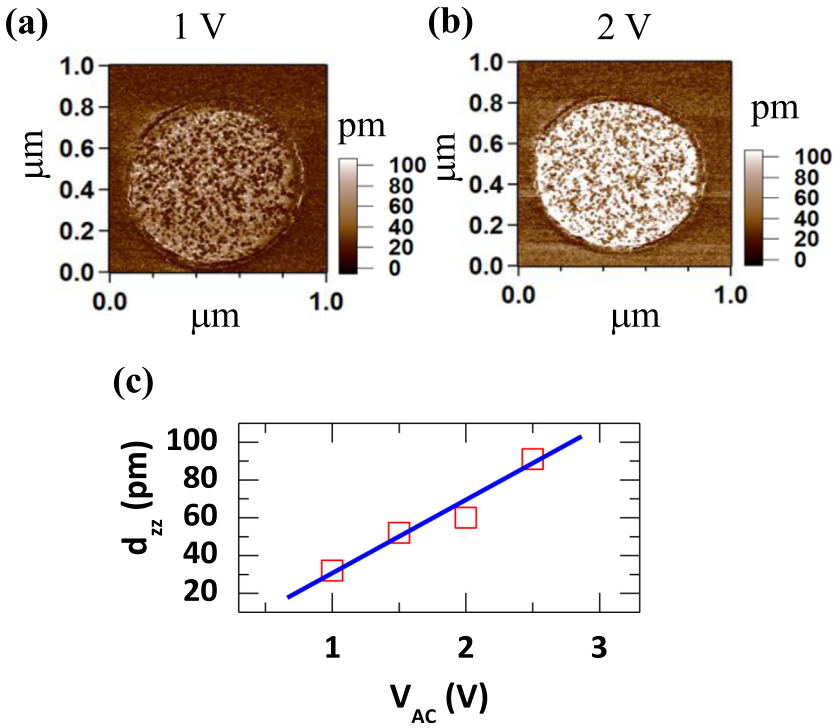

FIG. 3. Development of strain in nanoscaled MgO under the influence of applied *E*-field. (a) and (b) PFM images of the nanopillar device with 5 nm MgO at a.c. voltage amplitude of 1 V and 2 V. A strong development of strain can be seen at 2 V. (c) Strain coefficient (d_{zz}) values at different a.c. voltage amplitudes. A blue line indicates the linear dependence of d_{zz} with applied voltage.

strong strain in nanoscaled MgO. This *E*-field-induced strain effect is consistent with the theoretical calculation reported for the structurally distorted MgO at nanoscale, although the bulk MgO exhibits conventional dielectric properties.[32,33] It is worth to mention that the Cr_2O_3 also exhibits multiferroic orders at room temperature when it is in the form of epitaxial nano-clusters embedded in the MgO matrix, while it was absent in the bulk form.[35]

We have further investigated the effect of d.c. *E*-field polarity on the piezoresponse of nanoscaled MgO. PFM images were collected for a series of d.c. bias voltages ranging from −1.5 V to 1.5 V applied to a nanopillar. Figs. 4(a), 4(b), and 4(c) show the PFM images at $V_{DC} = 0$ V, −1.5 V, and +1.5 V, respectively. A distinct color contrast in the circular areas can be observed for applied voltage of different polarities, which is due to the effect of *E*-field polarity dependent induced-strain, i.e., the negative *E*-field induces a compressive strain (darker color), while the positive *E*-field induces a tensile strain (brighter) in nanoscaled MgO. In Fig. 4(d), we plot the d_{zz} as a function of V_{DC} which depicts the linear and polarity dependences of V_{DC}, which further confirms that the nanoscaled MgO behaves like a conventional piezoelectric material.

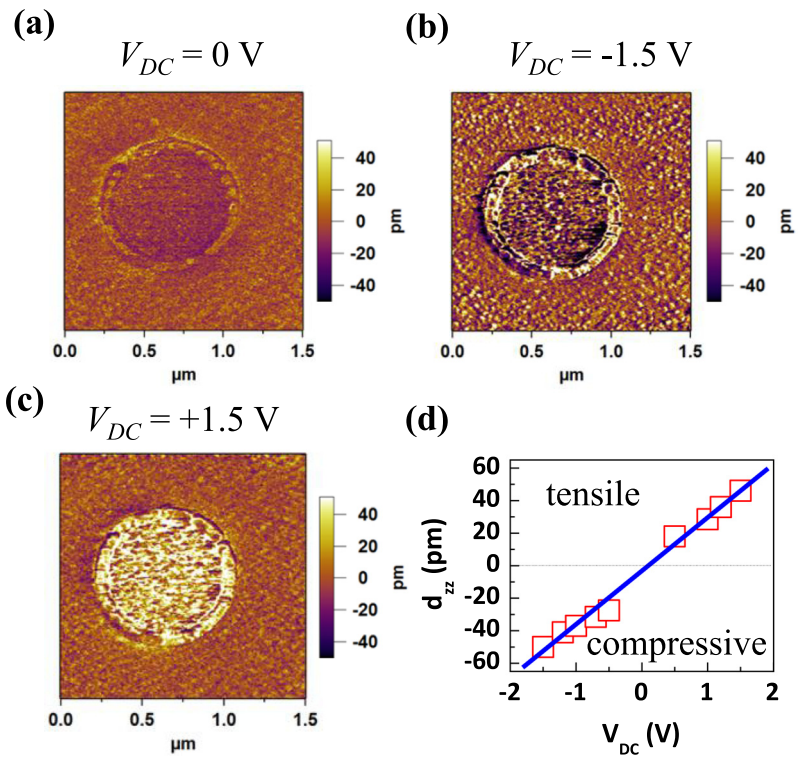

FIG. 4. Effect of d.c. *E*-field polarity on the piezoresponse of nanoscaled MgO. (a), (b), and (c) PFM images of a nanopillar device with 5 nm MgO under $V_{DC} = 0$, −1.5, and 1.5 V, respectively. Negative V_{DC} leads to compressive strain, while the positive V_{DC} gives rise to tensile strain. (d) d_{zz} values at different d.c. voltage amplitudes.

The demonstrated E-field dependent strain in the nanoscaled MgO could have a major role in altering the anisotropy field (H_k) of CoFeB magnetic layer in CoFeB-MgO MTJs through $H_k \propto \lambda_s \sigma$, where λ_s is the saturation magnetostriction and σ is the stress on the magnetic layer due to strain transfer from nanoscaled MgO. Unlike in the case of magnetic field and spin-transfer-torque switching of FL in MTJ, the magnetic anisotropy energy or barrier height (E_b) of a PMA MTJ ($E_b = \frac{1}{2} M_s H_k V$, where M_s–saturation magnetization and V–volume of the magnetic cell) is momentarily lowered under E-field. Since the charge density of a metal can be varied only slightly by E-field, the change in interfacial magnetic anisotropy energy due to the change in M_S is very small.[36] Therefore, the momentary reduction in E_b may be primarily attributed to the change in H_k under the influence of E-field. Indeed, the tuning of H_k by applying E-field is a common scheme in ME nanostructures which exhibit a ME coupling between the ferromagnetic/piezoelectric layers.[25–27] Recently, it has been shown that the E-field can significantly change the H_k of CoFeB layer when it is integrated with a conventional piezoelectric material due to strain-mediated ME coupling between the magnetostrictive CoFeB and piezoelectric layers.[37,38] The change of H_k under E-field due to ME coupling relies on the fact that the positive E-field strengthens the magnetization along the easy axis and the negative E-field tilts the magnetization from the easy axis. Both of these features are associated with the compressive and tensile strain transfer from the piezoelectric layer to a magnetostrictive layer. This kind of trend of E-field polarity dependent H_k change is similar to what we have observed in the E-field dependent PMA change in CoFeB/MgO MTJ as presented in Fig. 1(b), and also in the other reports.[18–20,34]

For a composite nanostructure exhibiting E-field induced strain-mediated cross interaction between the magnetostrictive effect in the ferromagnetic phase and piezoelectric effect in the ferroelectric/piezoelectric phase, the theoretical dependence of strain-induced H_k on the applied E-field is given by: $H_k = 3\lambda_s \eta \frac{Y}{1-\gamma} \frac{d_{zz}}{\mu_0 M_s} E$, where η is the mechanical coupling coefficient between ferromagnetic and ferroelectric/piezoelectric materials (from 0.5 to 1) and $\frac{Y}{1-\gamma}$ is the elastic modulus of ferromagnetic material, and E is the applied E-field. In the following, we have made a simple hypothesis that the E-field-induced strain in nanoscaled MgO generates a homogeneous strain in the whole CoFeB FL. We assume the perfect mechanical coupling between the CoFeB and MgO layers ($\eta = 1$), since the films are directly sputtered on top of one another. We take the value of $\frac{Y}{1-\gamma}$ is 200 N/m^2 and the value of λs is 2×10^{-5} for the ferromagnetic magnetostrictive CoFeB. The average value of d_{zz} for MgO determined from the PFM data (Fig. 3(c)) is found to be 37 pm/V. By considering above values, the change in the value of H_k for CoFeB for an applied E-field of $E = 1$ V/nm is found to be around 2340 Oe. Assuming the single domain switching, the change in the value of H_k of 2340 Oe is equivalent to a change in the thermal stability ($\Delta = E_b/k_bT$, where k_b is the Boltzmann constant and T is the temperature) value of approximately $\Delta = 52.8$ for $E = 1$ V/nm for a MTJ device of size 40 nm with 1.2 nm CoFeB FL. Based on the above values, the corresponding E-field efficiency (Δ/E) due to induced strain can be up to 52.8 (V/nm)$^{-1}$. It is worth to mention that the E-field efficiency calculated based on the strain-mediated effect in CoFeB/MgO is comparable with the experimentally determined E-field efficiency of 56 (V/nm)$^{-1}$ as reported by Wang *et al.* in CoFeB/MgO MTJs.[18]

In our recent work, using dynamical lock-in measurements[39] (similar to the technique[40] used for ME coefficient measurements in multiferroic/ME materials), we have observed that the frequency (f) response of E-field-induced a.c. voltage (V_{ac}) across CoFeB/MgO MTJ device in response to external a.c. magnetic field showed a peak around $f_{max} = 933$ Hz. Although it is suggested that the origin of E-field-induced V_{ac} is via TMR effect, the peak in frequency response of V_{ac} cannot be attributed to the TMR effect because TMR does not show such trend in such low frequency regime ($f \ll$ GHz, the ferromagnetic resonance frequency). However, it strongly signals the strain-mediated ME coupling between CoFeB/MgO layers under the influence of E-field, as the value of f_{max} found in our CoFeB/MgO system is close to the strain-mediated ME resonance frequency of 1197 Hz as reported in the similar magnetic system, CoFeBSi-based ME compound composed of a known piezoelectric material, AlN.[41] From the materials perspective, the only difference between the works reported in Refs. 41 and 39 is that the Ref. 41 uses a conventional piezoelectric material (AlN) and in Ref. 39 we used a normal dielectric material (MgO), while both CoFeBSi and CoFeB magnetic materials used are magnetostrictive. Thus, the strain-mediated ME effects observed in Ref. 41 is expectable even in the absence of E-field, whereas in Ref. 39 one would expect E-field-induced strain-mediated effect only if the nanoscaled MgO shows a piezo-response under the influence of E-field, and that is exactly the result we observed in this work using PFM measurements (Figs. 3 and 4). Moreover, a theoretical calculation by He and Chen,[42] also demonstrated that not only the applied E-field but also the variation in in-plane lattice strain can effectively change the PMA of CoFe FL to in-plane anisotropy in the CoFe/MgO MTJ system. Therefore, our results of E-field-induced strain (Fig. 3) and polarity dependent compressive and tensile strain (Fig. 4) observed in MgO nanostructures using PFM reveal that the E-field-induced strain effect in the confined CoFeB/MgO MTJ stack should contribute to the E-field-induced PMA change along with the known the phenomena of charge accumulation. However, a similar study of phase-field simulation using the time-dependent Ginzburg-Landau model as reported by Hu *et al.*,[43] in CoFeB-$BaTiO_3$ system, will be very useful to have a deeper understanding of the effect of E-field-induced strain in altering the PMA of CoFeB FL in CoFeB-MgO MTJs. Further investigation of the E-field-induced strain in nanoscaled MgO using photoluminescence experiments, and also the investigation of ME effect in CoFeB-MgO MTJs would be very interesting, and are well-deserved studies to quantify the E-field-induced strain-mediated ME coupling between the CoFeB and MgO layers.

In summary, we have presented a direct evidence for E-field-induced strain in nanoscaled MgO using PFM measurement. We have demonstrated the development of compressive and tensile strains in nanoscaled MgO which are corresponding to different polarities of applied E-field, and we have discussed its implication on the E-field controlled

PMA in CoFeB/MgO MTJs. Such *E*-field-induced strain effect represents a new avenue for exploring magnetoelectrically controlled spintronic devices so as to develop more energy-efficient spintronic devices.

[1]W. H. Butler, X. G. Zhang, T. C. Schulthess, and J. M. MacLaren, Phys. Rev. B **63**, 054416 (2001).
[2]J. Mathon and A. Umerski, Phys. Rev. B **63**, 220403 (2001).
[3]S. S. P. Parkin, C. Kaiser, A. Panchula, P. M. Rice, B. Hughes, M. Samant, and S.-H. Yang, Nat. Mater. **3**, 862 (2004).
[4]S. Yuasa, A. Fukushima, Y. Suzuki, and K. Ando, Nat. Mater. **3**, 868 (2004).
[5]S. Ikeda, K. Miura, H. Yamamoto, K. Mizunuma, H. D. Gan, M. Endo, S. Kanai, J. Hayakawa, F. Matsukura, and H. Ohno, Nat. Mater. **9**, 721 (2010).
[6]K. Yakushiji, T. Saruya, H. Kubota, A. Fukushima, T. Nagahama, S. Yuasa, and K. Ando, Appl. Phys. Lett. **97**, 232508 (2010).
[7]J. C. Slonczewski, J. Magn. Magn. Mater. **159**, L1 (1996).
[8]L. Berger, Phys. Rev. B **54**, 9353 (1996).
[9]D. C. Worledge, G. Hu, D. W. Abraham, J. Z. Sun, P. L. Trouilloud, J. Nowak, S. Brown, M. C. Gaidis, E. J. O'Sullivan, and R. P. Robertazzi Appl. Phys. Lett. **98**, 022501 (2011).
[10]S. Matsunaga, M. Natsui, S. Ikeda, K. Miura, T. Endoh, H. Ohno, and T. Hanyu, Jpn. J. Appl. Phys., Part 1 **50**, 063004 (2011).
[11]S. Matsunaga, J. Hayakawa, S. Ikeda, K. Miura, H. Hasegawa, T. Endoh, H. Ohno, and T. Hanyu, Appl. Phys. Express **2**, 023004 (2009).
[12]M. Tsujikawa and T. Oda, Phys. Rev. Lett. **102**, 247203 (2009).
[13]M. Weisheit, S. Faehler, A. Marty, Y. Souche, C. Poinsignon, and D. Givord, Science **315**, 349 (2007).
[14]T. Maruyama, Y. Shiota, T. Nozaki, K. Ohta, N. Toda, M. Mizuguchi, A. A. Tulapurkar, T. Shinjo, M. Shiraishi, S. Mizukami, Y. Ando, and Y. Suzuki, Nat. Nanotechnol. **4**, 158 (2009).
[15]M. Endo, S. Kanai, S. Ikeda, F. Matsukura, and H. Ohno, Appl. Phys. Lett. **96**, 212503 (2010).
[16]D. Chiba, M. Yamanouchi, F. Matsukura, and H. Ohno, Science **301**, 943 (2003).
[17]U. Bauer, M. Przybylski, J. Kirschner, and G. S. D. Beach, Nano Lett. **12**, 1437 (2012).
[18]W.-G. Wang, M. Li, S. Hageman, and C. L. Chien, Nat. Mater. **11**, 64 (2012).
[19]H. Meng, R. Sbiaa, M. A. K. Akhtar, R. S. Liu, V. B. Naik, and C. C. Wang, Appl. Phys. Lett. **100**, 122405 (2012).
[20]S. Kanai, M. Yamanouchi, S. Ikeda, Y. Nakatani, F. Matsukura, and H. Ohno, Appl. Phys. Lett. **101**, 122403 (2012).
[21]N. A. Pertsev, Sci. Rep. **3**, 2757 (2013).
[22]T. Kimura, T. Goto, H. Shintani, K. Ishizaka, T. Arima, and Y. Tokura, Nature **426**, 55 (2003).
[23]R. Ramesh and N. A. Spaldin, Nat. Mater. **6**, 21 (2007).
[24]Y. Tokunaga, Y. Taguchi, T. Arima, and Y. Tokura, Nat. Phys. **8**, 838 (2012).
[25]M. Fiebig, J. Phys. D: Appl. Phys. **38**, R123 (2005).
[26]J. Ma, J. Hu, Z. Li, and C. W. Nan, Adv. Mater. **23**, 1062 (2011).
[27]N. X. Sun and G. Srinivasan, Spin **2**, 1240004 (2012).
[28]R. Shimabukuro, K. Nakamura, T. Akiyama, and T. Ito, Physica E **42**, 1014 (2010).
[29]A. Manchon, J. Appl. Phys. **104**, 043914 (2008).
[30]M. T. Johnson, Rep. Prog. Phys. **59**, 1409 (1996).
[31]U. Bauer, S. Emori, and G. S. D. Beach, Nat. Nanotechnol. **8**, 411 (2013).
[32]A. N. Enyashin and A. L. Ivanovskii, Nanotechnology **18**, 205707 (2007).
[33]P. Gopal and N. A. Spaldin, J. Electron. Mater. **35**, 538 (2006).
[34]K. Kita, D. W. Abraham, M. J. Gajek, and D. C. Worledge, J. Appl. Phys. **112**, 033919 (2012).
[35]D. Halley, N. Najjari, H. Majjad, L. Joly, P. Ohresser, F. Scheurer, C. Ulhaq-Bouillet, S. Berciaud, B. Doudin, and Y. Henry, Nat. Commun. **5**, 3167 (2014).
[36]C. Fowley, K. Rode, K. Oguz, H. Kurt, and J. M. D. Coey, J. Phys. D: Appl. Phys. **44**, 305001 (2011).
[37]G. A. Lebedev, B. Viala, T. Lafont, D. I. Zakharov, O. Cugat, and J. Delamare, J. Appl. Phys. **111**, 07C725 (2012).
[38]N. Lei, S. Park, P. Lecoeur, D. Ravelosona, C. Chappert, O. Stelmakhovych, and V. Holý, Phys. Rev. B **84**, 012404 (2011).
[39]V. B. Naik, H. Meng, R. S. Liu, P. Luo, S. Yap, and G. C. Han, Appl. Phys. Lett. **104**, 232401 (2014).
[40]L. E. Fuentes-Cobas, J. A. Matutes-Aquino, and M. E. Fuentes-Montero, *Handbook of Magnetic Materials*, edited by K. H. J. Buschow (Elsevier, North Holland, 2011), Vol. 19, p. 161.
[41]E. Lage, C. Kirchhof, V. Hrkac, L. Kienle, R. Jahns, R. Kn€ochel, E. Quandt, and D. Meyners, Nat. Mater. **11**, 523 (2012).
[42]K. H. He and J. S. Chen, J. Appl. Phys. **111**, 07C109 (2012).
[43]J.-M. Hu, T. N. Yang, L. Q. Chen, and C. W. Nan, J. Appl. Phys. **113**, 194301 (2013).